EARTHQUAKE ENGINEERING AND STRUCTURAL DYNAMICS
Earthquake Engng. Struct. Dyn. **27**, 1013–1029 (1998)

MODELLING OF CONTRACTION JOINT AND SHEAR SLIDING EFFECTS ON EARTHQUAKE RESPONSE OF ARCH DAMS

DAVID T. LAU*,†, B. NORUZIAAN‡ AND A. G. RAZAQPUR§
Department of Civil and Environmental Engineering, Carleton University, Ottawa, Ont., Canada K1S 5B6

SUMMARY

In an arch dam, adjacent monoliths separated by vertical contraction joints may move relative to each other during an earthquake, resulting in the gradual opening and closing and possible shear movement at the joint surfaces. This paper presents the formulation of a joint constitutive model for a zero-thickness joint element that can simulate both the opening and closing and shear sliding behaviour, as well as the non-linear shear key effects of the joint. The proposed joint element has been implemented in the concrete arch dam finite element analysis program ADAP-88. The response of a typical arch dam subjected to earthquake ground motion is presented to demonstrate the capability of the proposed joint model. Results from a parametric study carried out to study the sensitivity of the response to the joint properties are discussed. The joint parameters considered in the parametric study include apparent cohesion, friction coefficient, and whether the joint has beveled or unbeveled shear key, or the joint is unrestrained in shear sliding. The analysis results show that joint opening and shear slippage at the contraction joints can have significant effects on the response of an arch dam. © 1998 John Wiley & Sons, Ltd.

KEY WORDS: arch dam; contraction joints; non-linear finite element; earthquake response; shear keys; shear sliding

INTRODUCTION

Concrete is a brittle material and is susceptible to cracking due to its low tensile strength. To avoid the development of tensile stresses due to shrinkage and temperature drop in mass concrete, arch dams are built as assemblages of monoliths separated by vertical contraction joints, as shown in Figure 1.

In an arch dam located in an area of high seismicity, adjacent monoliths may move relative to each other during an earthquake, resulting in the opening and closing of the joints and possible shear movement at the joint surfaces. Under static conditions, the joints are under compression due to the hydrostatic pressure from the reservoir and these static compressive forces are transmitted along the arch axis to the abutments at the ends of the dam. The dynamic response during an earthquake generally imposes additional alternating compressive and tensile loads on the joints, and if the latter loads are more than the static compressive force, the joint will open up. A significant portion of the tensile force will then be released in the arch direction, making the structure more flexible, and possibly resulting in the overstress of the monoliths in the cantilever direction due to the redistribution of forces from the arch to the cantilever direction. On the other hand, for a partially opened joint, the resulting reduction in the load-bearing area of the joint may lead to compressive failure of the adjacent concrete.

* Correspondence to: David T. Lau, Department of Civil and Environmental Engineering, Carleton University, 3432 C.J. Mackenzie Building, Ottawa, Ontario, Canada K1S 5B6. E-mail: dtl@ritz.carleton.ca
† Associate Professor
‡ Former doctoral student
§ Professor

Contract/grant sponsor: Natural Sciences and Engineering Reasearch Council of Canada
Contract/grant sponsor: Ministry of Higher Education of Iran

CCC 0098–8847/98/101013–17$17·50

Received 30 April 1996
Revised 10 February 1998

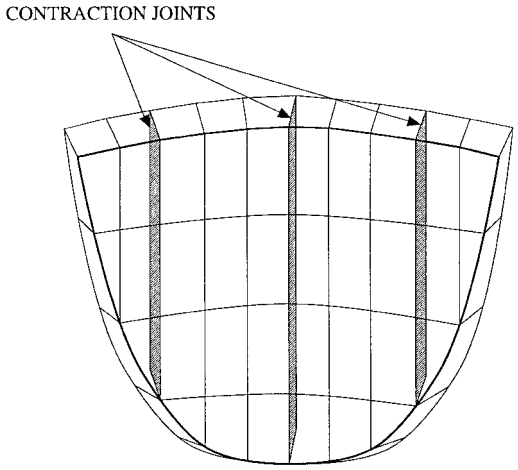

Figure 1. Vertical contraction joints in an arch dam

It is common practice in arch dams located in seismic active regions to have shear boxes or shear keys at contraction joints, which together with friction effect the transfer of shear between the monoliths. Shear keys can be either beveled or unbeveled.

In recent years, extensive research has been carried out by many researchers to study the behaviour of arch dams under static and dynamic loads.[1–12] Among these, a number of researchers have studied the effect of contraction joints on the seismic response of arch dams. Niwa and Clough[13] conducted a series of experiments on a segmented arch rib model and a cantilever monolith subjected to typical earthquake ground motions. Results of the test showed that opening of the joints limits the development of the tensile stress in the arch direction and changes the natural vibrational period of the structure.

Based on numerical study of the joint behaviour, Dowling and Hall[14] developed a special method to model the gradual opening and closing of the joint with no-slip. Results of their study on the behaviour of the Pacoima Dam showed that the large separations at the contraction joints near the top of the dam may violate the no slip assumption, particularly at un-keyed joints without sufficient frictional resistance. Their results also indicated the possible formation of crack in the cantilever direction due to loads transferred from the arch direction, precipitated by the opening of the vertical contraction joints. Similar conclusions were reached by Taskov and Jurukovski[15] in their study of a dam central cantilever monolith bounded by two neighbouring blocks. In another study, Weber *et al.*[16] investigated the non-linear behaviour of arch dams with keyed joints of infinite strength. Although valuable information on the behaviour of arch dams was obtained, the infinite strength joint assumption prevented any phase difference between the motions of adjacent cantilevers, and thus may have stabilized the dam structure to the extent that no critical bending stress could develop.

Recently, Hohberg[17] implemented a rather detailed joint model using generalized non-linear springs to represent joint behaviour. The model considered frictional slippage, slippage due to separation and the asperity of the joint surfaces. However, in the modelling of the shear keys, the effect of the shear keys was considered approximately by increasing the height of the joint asperity. In a direct modelling approach, Fenves *et al.*[18–20] developed a discrete three-dimensional non-linear joint element. The model could simulate the gradual opening and closing behaviour of the joint. But the relative tangential displacements of the joints were not allowed in the formulation. The element was implemented in an efficient substructuring solution procedure. Results of their study gave valuable insight into the non-linear behaviour of arch dams during earthquakes. The results clearly showed the transfer of stresses from the arch to the cantilever direction when the joints opened, and that the joint-opening behaviour is dependent on the presence of keys in the contraction joints.

The above literature survey reveals a gap in knowledge pertaining to the seismic response analysis of arch dams. There is need for a joint model that can simulate both the opening–closing and non-linear shear slippage behaviour at the contraction joints, as well as the shear key effects. This paper presents the development of such a new joint model and its implementation in a finite element analysis procedure for arch dams. A parametric study of a typical arch dam subjected to earthquake ground motions is presented to demonstrate the capability of the proposed joint model and the sensitivity of the dam structural response to the joint properties. It is recognized that the calibration of the model parameters would require test results, but nevertheless the model could be used as a useful analytical tool to assess the non-linear seismic behaviour of arch dams.

MODELLING OF CONTRACTION JOINTS

Modelling of joints for elastic, plastic and for cyclic load effects have been conducted by many researchers.[21–26] Here a more comprehensive joint model is proposed for arch dams.

The contraction joints are modelled by zero-thickness joint elements. The tangential displacement in the joint plane has two orthogonal components. The shear displacement and shear stress associated with slippage of the joint are expressed in terms of the resultant of the two components. The magnitude and direction of the resultant shear displacement and shear stress change continuously throughout the response. Loading and unloading of the joint shear is represented by the change in the magnitude of the resultant shear stress.

A shear key is modelled by specifying an appropriate limit on the relative shear displacement between the joint faces. In general, a shear key that is not beveled prevents slippage before the joint is fully open whereas in the case of beveled shear keys, the two faces of the joint can have limited slippage when the joint is only partially open. In the present study, this kind of slippage or sliding behavior during partial opening of beveled shear keys is not explicitly considered in the formulation. However, for small shear slippage, the sliding behaviour of a bevel-keyed joint during partial opening may be considered close to that of an un-keyed joint. The proposed joint constitutive model can take into account the strength of the shear key in the contraction joint. The non-linear effect of the initial yielding or crushing of the shear key on the performance of the arch dam is accounted for by using an appropriate value for the joint apparent cohesion modelling parameter to represent the strength of the shear key.

The contraction joint is modelled by several eight-node joint elements (with 4 double nodes) with 2×2 Gaussian integration through the thickness of the dam. The element consists of two adjacent surfaces that are completely coincident with each other during the initial at rest condition. The kinematics of the element are expressed in terms of the relative displacements of the two faces of the joint.

The following basic assumptions are made in the derivation of the constitutive model for the proposed joint element. The assumptions are based on the expected behaviour of joints under seismic excitation: (1) The joint has negligible tensile strength; (2) The joint tangential stiffness will be reduced to zero when the joint is completely open, as defined by the joint normal relative displacement exceeding a pre-defined slip margin δ; (3) The normal stress and normal stiffness in an open joint are reduced to zero; (4) The joint behaves elastically in sliding when the joint is open, provided the shear stress is less than the shear strength or apparent cohesion of the joint; (5) In the partial open state, when the shear stress exceeds the shear strength limit of the joint, further sliding of the joint is resisted by a constant shear force resulting from apparent cohesion; (6) There is no coupling between the normal and shear displacements when the joint is open and the normal stress remains zero; (7) When the joint is closed, the friction between the two faces of the joint becomes effective in resisting the sliding motion. The joint behaves elastically or elasto-plastically, with coupling between the shear and the normal displacements; (8) The joint faces are assumed to be isotropic; (9) The plasticity model for sliding is assumed to be of the Mohr–Coulomb type and governed by an associative flow rule. (10) There is no mismatch in the shear keys upon closing of the opened joints in the displaced state of the dam.

The proposed joint model is implemented in the computer program ‘BANDAAB’, developed at Carleton University. ‘BANDAAB’ is an extension of the computer program ‘ADAP88’ developed at the University of

California at Berkeley, which already has a joint element with the capability of modelling the opening–closing non-linear behaviour.[1,18] In the following, the formulation and numerical implementation of the proposed joint model, which also includes the shear slippage and shear key effects, are described.

JOINT BEHAVIOUR IN CLOSED STATE

For analysis of the non-linear seismic response of arch dams, the direct time step integration method is followed. Considering the response of the dam structure to be known at the end of time step m, the corresponding stress and strain vectors, $\boldsymbol{\sigma}_m$ and $\boldsymbol{\varepsilon}_m$, are used as the initial conditions for the iteration in the next time step $(m+1)$.

In the numerical formulation of the proposed zero thickness joint element, the relative displacements at the integration points, instead of the strains, are used in the constitutive formulation. For a joint that behaves elastically in the closed state, the implemented constitutive relations can be expressed as follows:

$$(\Delta\sigma^{\mathrm{e}})^{i}_{m+1} = k_{\mathrm{n}}(\Delta v)^{i}_{m+1} \tag{1}$$

$$(\Delta\tau^{\mathrm{e}}_1)^{i}_{m+1} = k_{\mathrm{s}}(\Delta u_1)^{i}_{m+1} \tag{2}$$

$$(\Delta\tau^{\mathrm{e}}_2)^{i}_{m+1} = k_{\mathrm{s}}(\Delta u_2)^{i}_{m+1} \tag{3}$$

where $(\Delta\sigma^{\mathrm{e}})^{i}_{m+1}$, $(\Delta\tau^{\mathrm{e}}_1)^{i}_{m+1}$ and $(\Delta\tau^{\mathrm{e}}_2)^{i}_{m+1}$ are, respectively, the elastic part of the incremental normal and tangential (shear) stresses at the ith iteration of time step $(m+1)$, $(\Delta v)^{i}_{m+1}$, $(\Delta u_1)^{i}_{m+1}$ and $(\Delta u_2)^{i}_{m+1}$ are the current incremental relative normal and tangential displacements of the joint. Subscripts '1' and '2' denote the two orthogonal tangential displacement directions in the plane of the joint. Parameters k_{n} and k_{s} are penalty parameters which, respectively, simulate the no penetration condition of the joint faces, and the stick or no slippage condition in the joint plane.

As mentioned before, the joint slippage in the closed state is resisted by friction and cohesion. Hence, similar to Hohberg,[25] a two-dimensional Mohr–Coulomb model is adopted to simulate the joint slippage behaviour in the closed state. The loading function f in the contact stress space is written as

$$f = \tau + \mu\sigma - c \tag{4}$$

$$\tau = \sqrt{\tau_1^2 + \tau_2^2} \tag{5}$$

$$\mu = \tan\phi \tag{6}$$

where τ_1 and τ_2 are the components of the shear stress in two perpendicular directions on the contact surface, σ is the normal stress which is assumed to be positive in tension, ϕ is the friction angle and c is the apparent cohesion of the joint.

Once the joint exceeds its elastic limit, further sliding will follow an elasto-plastic behaviour, that is

$$\{\Delta\mathbf{u}\} = \{\Delta\mathbf{u}^{\mathrm{e}}\} + \{\Delta\mathbf{u}^{\mathrm{p}}\} \tag{7}$$

where $\Delta\mathbf{u}$ is the increment of the total relative displacement vector of the joint and superscripts 'e' and 'p' denote elastic and plastic contributions. When the sheared-off element is in a state of sliding, and assuming the flow rule to be associative, the behaviour is treated as perfectly plastic and the constitutive equations are written as

$$\begin{Bmatrix} \Delta\sigma \\ \Delta\tau_1 \\ \Delta\tau_2 \end{Bmatrix} = [\mathbf{D}_{\mathrm{ep}}] \begin{Bmatrix} \Delta v \\ \Delta u_1 \\ \Delta u_2 \end{Bmatrix} \tag{8}$$

where the elastoplastic rigidity matrix $[\mathbf{D}_{ep}]$ is given by

$$[\mathbf{D}_{ep}] = \begin{pmatrix} k_n - \frac{1}{H}\mu^2 k_n^2 & -\frac{1}{H}k_n k_s \beta_1 \mu & -\frac{1}{H}k_n k_s \beta_2 \mu \\ -\frac{1}{H}k_n k_s \beta_1 \mu & k_s(1 - \frac{1}{H}k_s \beta_1^2) & -\frac{k_s^2}{H}\beta_1 \beta_2 \\ -\frac{1}{H}k_n k_s \beta_2 \mu & -\frac{k_s^2}{H}\beta_1 \beta_2 & k_s(1 - \frac{1}{H}k_s \beta_2^2) \end{pmatrix} \tag{9}$$

$$H = k_n \mu^2 + k_s \beta_1^2 + k_s \beta_2^2 = k_n \mu^2 + k_s \tag{10}$$

$$\beta_1 = \frac{\partial f}{\partial \tau_1} = \frac{\tau_1}{|\tau|} \tag{11}$$

$$\beta_2 = \frac{\partial f}{\partial \tau_2} = \frac{\tau_2}{|\tau|} \tag{12}$$

$$\mu = \frac{\partial f}{\partial \sigma} \tag{13}$$

The off-diagonal terms in the matrix $[\mathbf{D}_{ep}]$ reflect the phenomena of shear dilatancy and slip circle.

The loading or unloading status of the joint from a plastic state is determined from the plastic work of the joint element

$$\Delta w_p = \sigma \Delta v^p + \tau_1 \Delta u_1^p + \tau_2 \Delta u_2^p \tag{14}$$

When the increment of the plastic work Δw_p is non-negative, the joint is in a state of loading, whereas for the case of equation (14) is negative, the joint is unloading.

The stress states at all the integration points within a finite element are checked to determine whether the material at each of the integration points is under elastic loading, plastic loading, or unloading. For the integration point that is already in an elastoplastic state at the end of time step m, the loading criterion function L obtained from the increment of the yield function $\{\partial f/\partial \boldsymbol{\sigma}\}^T[\mathbf{D}_e]\{\Delta \mathbf{u}\}$ is evaluated

$$L = k_n \mu (\Delta v)_{m+1}^i + k_s (\beta_1)_m (\Delta u_1)_{m+1}^i + k_s (\beta_2)_m (\Delta u_2)_{m+1}^i > 0 \tag{15}$$

If the condition in equation (15) is satisfied, the joint is in a loading state, and the stress increments are calculated with the elastoplastic rigidity matrix. Otherwise, the joint is unloading with the elastic joint stiffness.

On the other hand, if the integration point is in an elastic state at the end of time step m, the current stress state is first calculated assuming the behaviour to remain elastic. If $f(\boldsymbol{\sigma}_{m+1}^i) < 0$, the integration point remains elastic, and the calculated stress state is correct. Otherwise, for $f(\boldsymbol{\sigma}_{m+1}^i) \geqslant 0$, the stress point is considered to be elastoplastic for the current iteration. To account for overshooting the loading surface, as a result of the material changing from an elastic state to a plastic state, a scale factor r is defined and utilized to bring the stress state back onto the loading surface, such that $f(\{\boldsymbol{\sigma}\}_m + r\{\Delta \boldsymbol{\sigma}^e\}_{m+1}^i) = 0$. The scale factor r is calculated by the following equation:

$$r = \frac{-[(\sigma)_m \mu + \sqrt{(\tau_1^2)_m + (\tau_2^2)_m} - c]}{[\mu(\Delta \sigma^e)_{m+1}^i + (\beta_1)_m (\Delta \tau_1^e)_{m+1}^i + (\beta_2)_m (\Delta \tau_2^e)_{m+1}^i]} \tag{16}$$

The current stress state thus becomes

$$\{\Delta \boldsymbol{\sigma}\}_{m+1}^i = r\{\Delta \boldsymbol{\sigma}^e\}_{m+1}^i + \int_{\{\mathbf{u}\}_m + r\{\Delta \mathbf{u}\}_{m+1}^i}^{\{\mathbf{u}\}_m + \{\Delta \mathbf{u}\}_{m+1}^i} [\mathbf{D}_{ep}]\{d\mathbf{u}\} \tag{17}$$

The integral in equation (17) is evaluated numerically. The integration interval is sub-divided into k sub-intervals. The displacement sub-increment for each sub-interval is calculated as follows

$$(\Delta \tilde{v})_{m+1}^i = \frac{1 - r}{k} (\Delta v)_{m+1}^i \tag{18}$$

$$(\Delta\tilde{u}_1)^i_{m+1} = \frac{1-r}{k}(\Delta u_1)^i_{m+1} \tag{19}$$

$$(\Delta\tilde{u}_2)^i_{m+1} = \frac{1-r}{k}(\Delta u_2)^i_{m+1} \tag{20}$$

The numerical integration procedures are repeated k times for the number of sub-intervals considered. The number of k sub-intervals used to evaluate the plastic strain increment depends on the size of the integration time step adopted in the dynamic response analysis of the arch dam. In the study reported here, a value of 20 is selected for k, which is significantly higher than the minimum number of sub-intervals required for accurate results. From the elastoplastic constitutive relation in equation (8), the plastic displacement sub-increments, denoted by the superscript '~', for the jth sub-interval can be determined as follows:

$$\{\Delta\tilde{\mathbf{u}}^{\mathrm{p}}\}^i_{(m+1),j} = \mathbf{P}^i_{(m+1),j}\{\Delta\tilde{\mathbf{u}}\}^i_{(m+1),j} \tag{21}$$

where

$$\mathbf{P}^i_{(m+1),j} = \frac{1}{(k_{\mathrm{s}} + k_{\mathrm{n}}\mu^2)} \begin{pmatrix} k_{\mathrm{n}}\mu^2 & k_{\mathrm{s}}\mu\beta_1 & k_{\mathrm{s}}\mu\beta_2 \\ k_{\mathrm{n}}\mu\beta_1 & k_{\mathrm{s}}(\beta_1)^2 & k_{\mathrm{s}}\beta_1\beta_2 \\ k_{\mathrm{s}}\mu\beta_2 & k_{\mathrm{s}}\beta_1\beta_2 & k_{\mathrm{s}}(\beta_2)^2 \end{pmatrix}^i_{(m+1),(j-1)} \tag{22}$$

which indicates that the determination of the plastic displacement sub-increment in the current jth sub-interval uses the flow gradient in the previous $(j-1)$th sub-interval. Now, the elastic stress sub-increments may then be calculated as follows:

$$(\Delta\tilde{\sigma}^{\mathrm{e}})^i_{(m+1),j} = k_{\mathrm{n}}(\Delta\tilde{v} - \Delta\tilde{v}^{\mathrm{p}})^i_{(m+1),j} \tag{23}$$

$$(\Delta\tilde{\tau}^{\mathrm{e}}_1)^i_{(m+1),j} = k_{\mathrm{s}}(\Delta\tilde{u}_1 - \Delta\tilde{u}^{\mathrm{p}}_1)^i_{(m+1),j} \tag{24}$$

$$(\Delta\tilde{\tau}^{\mathrm{e}}_2)^i_{(m+1),j} = k_{\mathrm{s}}(\Delta\tilde{u}_2 - \Delta\tilde{u}^{\mathrm{p}}_2)^i_{(m+1),j} \tag{25}$$

The new stress state in the current time step is given by the sum of the contributions from all the sub-increments

$$\boldsymbol{\sigma}^i_{(m+1)} = \boldsymbol{\sigma}^i_{(m)} + \sum_{j=1}^{k}(\Delta\tilde{\boldsymbol{\sigma}}^{\mathrm{e}})^i_{(m+1),j} \tag{26}$$

During the process of plastic loading, the consistency condition $df = 0$ of the stress state may be violated. If this occurs, the final stress state should be brought back to the loading surface. This is achieved by adding to the stress state a corrective stress increment that is normal to the loading surface. The corrected stress state thus becomes

$$\begin{Bmatrix} \sigma \\ \tau_1 \\ \tau_2 \end{Bmatrix}^i_{m+1(\mathrm{cor.})} = \begin{Bmatrix} \sigma \\ \tau_1 \\ \tau_2 \end{Bmatrix}^i_{m+1} + a \begin{Bmatrix} \mu \\ \beta_1 \\ \beta_2 \end{Bmatrix}^i_{m+1} \tag{27}$$

where the scalar factor a is determined by expanding the loading function f in Taylor's series form

$$a = \frac{-f^i_{m+1}}{(\mu^2+1)} = \frac{-1}{(\mu^2+1)}(\mu\sigma + \sqrt{(\tau_1^2+\tau_2^2)} - c)^i_{m+1} \tag{28}$$

JOINT BEHAVIOUR IN OPEN STATE

For an open joint, that is when the normal relative displacement v is positive, a threshold slip margin δ is defined to model the height of the shear keys. In the formulation, whenever the slip margin is exceeded, the tangential penalty parameter is reduced. The slip margin and the amount of the penalty reduction depend on whether the joint is keyed or un-keyed and whether the key is beveled or not.

The normal stiffness behaviour of the joint is shown in Figure 2(a). The normal stiffness of the joint is reduced to zero so that no stress is transferred between the two faces of the joint when it is open. When the joint is closed again with $v \leqslant 0{\cdot}0$, the stiffness of the joint recovers fully.

Typical sliding behaviour of the joint is presented in Figure 2(b). The behaviour is elastic when the shear stress is less than the limiting value c. For an un-keyed joint, c is the assumed apparent cohesion, and is

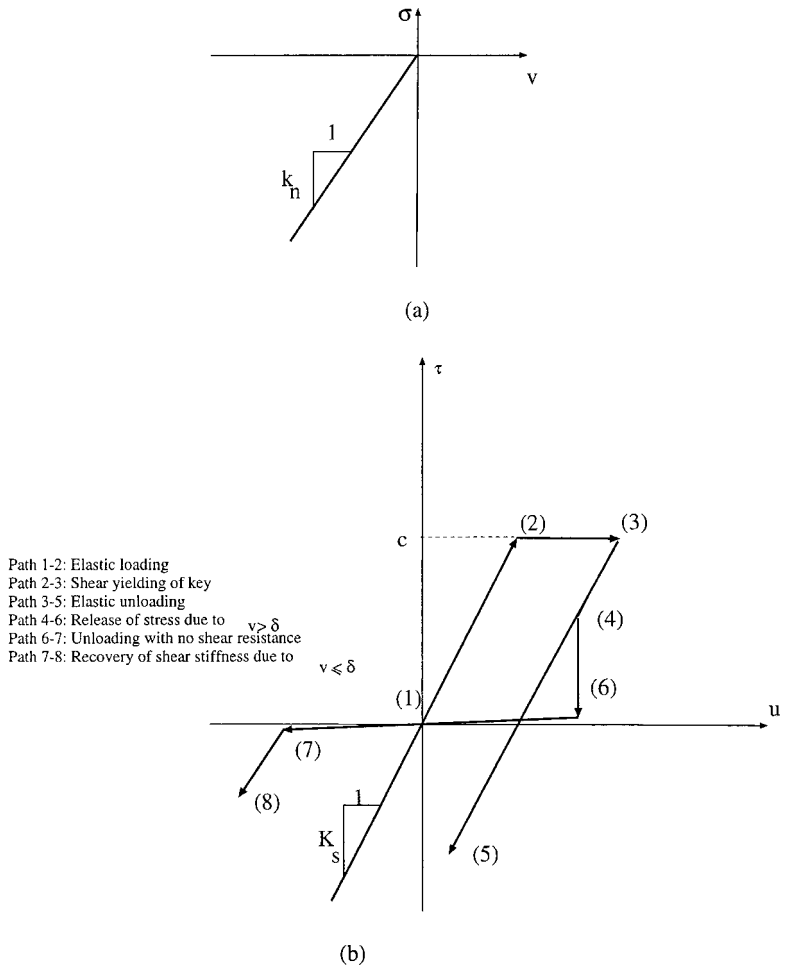

Figure 2. Constitutive relations of nonlinear joint element

much smaller than in a keyed joint, whence c represents the shear or bearing strength of the keys. Exceeding this limit, the joint will slide with constant shear resistance and its unloading would be elastic. The sudden release of the shear stress, due to the relative normal displacement v of the joint opening greater than the slip margin δ, is indicated by the path 4–6 in Figure 2(b). In the model the latter behaviour can be simulated by rendering the tangential penalty parameter k_s zero. In the present study, however, k_s is reduced to a small number close to zero in a fully open joint to avoid numerical problems in convergence, especially when the slip margin δ is small and close to zero, as illustrated by the very small slope of the path 6–7 in Figure 2(b). The reduction in the strength of the shear key due to accumulated damage and brittle crushing failure of the shear key are not considered in the present study.

When it is determined that the joint is open at an integration point, that is when $v^i_{m+1} > 0$, the normal stress σ^i_{m+1} is set equal to zero. Furthermore, if the normal relative displacement v^i_{m+1} is determined to be greater than the prescribed slip margin δ, that is the opening of the joint is larger than the height or depth of the shear key, the shear stresses $(\tau_1)^i_{m+1}$ and $(\tau_2)^i_{m+1}$ of the joint are also set equal to zero. But if v^i_{m+1} is less than δ, the shear key is assumed to be still engaged. The tangential displacement increments are then calculated. Assuming elastic behaviour in the sliding of the joint, the current tangential stresses are obtained. If at the end of the present iteration the resultant tangential stress $\tau^i_{m+1} \geqslant c$, the strength of the shear key is exceeded which signifies that the shear key element has yielded, and the tangential stresses are then limited to the yielding strength of the shear key as follows:

$$\tau_1 = \frac{\tau^i_{1m+1}}{\tau^i_{m+1}} c \tag{29}$$

$$\tau_2 = \frac{\tau^i_{2m+1}}{\tau^i_{m+1}} c \tag{30}$$

This completes the joint model which is implemented in a non-linear finite element program.

DYNAMIC EQUATIONS OF MOTION

The dynamic analysis and modelling procedures in the present investigation are based on ADAP88, which are briefly described here. In the analysis, the arch dam and its foundation are modelled by finite elements. The vertical contraction joints in the dam body are modelled by the proposed joint element, whereas the dam body between the contraction joints is discretized by a refined mesh of linear 3D solid elements in the vicinity of the joints and by thick shell elements away from the joints. The kinematic interaction effect between the arch dam and the supporting foundation rock is considered in the analysis by the foundation rock of depth equal to the height of the dam. The rock is modelled by an assemblage of linear elastic massless 3D solid elements. The inertia effects from the propagation of the seismic waves through the foundation rock are neglected in the massless model.

The hydrodynamic fluid–structure interaction effects between the dam and the water impounded in the reservoir are considered through the added mass concept. The water is assumed to be incompressible and inviscous. The pressure of this ideal fluid is governed by the Laplace's equation. Although previous studies have shown that water compressibility affects the earthquake response of arch dams,[3–5] the compressibility effects are not considered in the present study because the required frequency-domain solution procedure to include the frequency-dependent hydrodynamic effects precludes the non-linear effects of joint opening and shear sliding. On the dam–water interface, continuity of the normal acceleration of the dam and the fluid is established. The reservoir truncated boundary is taken at a distance twice the dam height, at which the acceleration is assumed to be zero. In conformity with the original ADAP88 program, the diagonalization procedures of the added mass matrix by Kuo[27] are followed.

The non-linearity of the arch dam reservoir–foundation system is localized at the contraction joints. The substructuring modelling techniques are employed in the modelling of the linear part of the dam and foundation

rock. Using equilibrium and compatibility conditions at the boundaries of the substructures, the influences of the linear substructures are condensed to the degrees of freedom at the boundaries with non-linear substructures of the contraction joints. As the location of the non-linearities in the system are known, the substructuring techniques used greatly reduces the amount of computation required in the iterative solution of the non-linear equations of motion of the arch dam–reservoir–foundation rock system.

The equations of motion for the non-linear part of the system can be expressed as follows:

$$\mathbf{M}\ddot{\mathbf{U}}_{n+1} + \mathbf{P}(\dot{\mathbf{U}}_{n+1}, \mathbf{U}_{n+1}) = \mathbf{F}_{n+1} + \mathbf{Q}_{n+1} \tag{31}$$

where $\mathbf{U}_{n+1}$, $\dot{\mathbf{U}}_{n+1}$ and $\ddot{\mathbf{U}}_{n+1}$ are, respectively, the displacement, velocity and acceleration vector at time t_{n+1}, and $\mathbf{M}$ is the mass matrix, $\mathbf{P}$ is the restoring force which is a non-linear function of the velocities and displacements, $\mathbf{F}_{n+1}$ is the time-dependent external load vector, and finally $\mathbf{Q}_{n+1}$ is the vector of forces from the linear substructures acting on the boundary of the non-linear substructure (contraction joints). The equations of motion are solved by the iterative direct time step integration Newmark β method with the constants $\beta = 0{\cdot}36$ and $\gamma = 0{\cdot}7$ and a time step of $0{\cdot}005$ s. For the iterative solution of the equations of motion, the Newton–Raphson or modified Newton–Raphson method using the tangent stiffness, secant or initial stiffness method may be used. For the proposed joint element, it is found that the initial stiffness approach generally leads to a more stable convergence in the response. The tangential stiffness and penalty parameters in some cases caused non-convergence and oscillation of the results. Typically, the time step integration converges in less than 20 iterations. The incremental form of the matrix equilibrium equation can be expressed as follows:

$$\mathbf{K}^* \Delta \mathbf{U} = \Delta \mathbf{P}^* \tag{32}$$

where the effective stiffness matrix $\mathbf{K}^*$ and the out-of-balance load vector $\Delta \mathbf{P}^*$ are given as follows:

$$\mathbf{K}^* = a_1 \mathbf{M} + a_2 \mathbf{C}_\mathrm{T} + \mathbf{K}_\mathrm{T} + \sum \bar{\mathbf{k}}^* \tag{33}$$

$$\Delta \mathbf{P}^* = \mathbf{F}_{n+1} - \mathbf{M}\ddot{\mathbf{U}}^k_{n+1} - \mathbf{P}(\dot{\mathbf{U}}^k_{n+1}, \mathbf{U}^k_{n+1}) + \sum \bar{\mathbf{p}}^*_{n+1} - \sum \bar{\mathbf{k}}^* \mathbf{u}_{\mathrm{b}}{}^k_{n+1} \tag{34}$$

where $\mathbf{C}_\mathrm{T}$ and $\mathbf{K}_\mathrm{T}$ are the tangent damping and tangent stiffness matrices of the non-linear substructure, and $\bar{\mathbf{k}}^*$ and $\bar{\mathbf{p}}^*_{n+1}$ are, respectively, the condensed effective stiffness matrix and condensed effective load vector from the linear elastic body of the dam and the foundation substructure, $\mathbf{u}_\mathrm{b}$ is the displacement vector at the boundary interface between the linear and non-linear substructures. The superscript k denotes the kth iteration within the considered time step for the incremental solution.

PARAMETRIC STUDY

In this section the effects of contraction joint movements on the seismic behaviour of a typical arch dam are discussed. To study the effects of the constitutive parameters of the proposed model, the behaviour of the Morrow Point Dam subjected to ground motions in the upstream and vertical directions, shown in Figure 3, is investigated. Figure 4 shows the typical finite element mesh used to model half of the dam body. In the analyses, the modulus of elasticity of concrete is taken as 23·9 GPa, the Poisson's ratio as 0·20, and the mass density as 2070 kg/m^3. For the foundation material, The modulus of elasticity is 15·9 GPa, and the Poisson's ratio is 0·20. Damping of the system is assumed to be of the Rayleigh type with 5 per cent damping in the first and fifth vibration modes of the dam with empty reservoir. But in the earthquake response analyses, the reservoir is assumed to be full so as to produce the maximum inertial effect from the reservoir liquid content.

The three joint characteristic parameters in the proposed model, as discussed earlier, are the slip margin δ, the apparent cohesion c, and the friction angle ϕ. Six cases were studied to verify the implementation of the proposed joint model and to investigate the effects of the joint parameters on the slippage behaviour of the arch dam during an earthquake. These are summarized in Table I. Case 1 simulates the behaviour of contraction joints with very large and strong un-beveled shear keys grouted with high friction grouting material. This

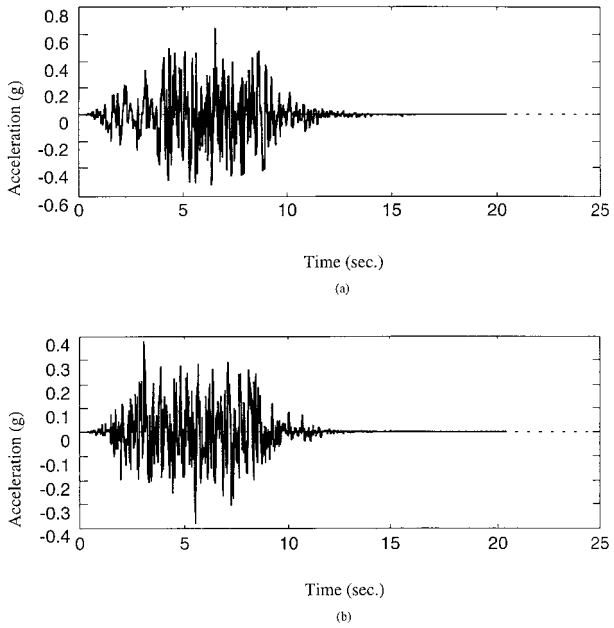

Figure 3. (a) Upstream and (b) vertical components of input ground motion

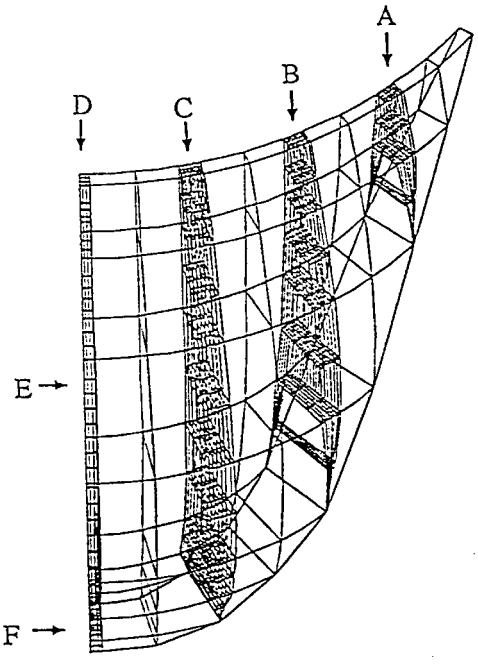

Figure 4. Finite element mesh of half dam body of Morrow Point Dam

Table I. Case for parametric study of contraction joints and shear key sliding effects

Case No.	Slip margin δ (cm)	Apparent cohesion (c)	Friction angle (ϕ)	Remarks
1	320(∞)	$10f_c'$	90°	Large and strong key, high friction
2	320(∞)	$0{\cdot}1f_c'$	90°	Large key with moderate strength, high friction
3	320(∞)	$0{\cdot}1f_c'$	45°	Large key with moderate strength, moderate friction
4	0.3	$10f_c'$	90°	No key or beveled key, large shear resistance
5	0.3	$0{\cdot}1f_c'$	45°	No key or beveled key, moderate shear resistance
6	0.3	$0{\cdot}1f_c'$	25°	No key or beveled key, low shear resistance

simulates the baseline reference case of total restraint of slippage at the contraction joints by the selection of a very large slip margin of 320 cm and a friction angle of 90° (infinite friction capacity), thus totally eliminating the possibility of shear slippage due to complete opening of the joint. It is noted here that in reality, the friction angle of the joint is limited by the internal friction angle of the grout material. Case 2 represents the case of contraction joints with very large un-beveled shear keys of limited strength, thus allowed to yield, and high friction grouting material. Case 3 simulates a situation where very large un-beveled shear keys are built, but the strength of the keys and the frictional resistance of the grout material are limited. Case 4 allows slippage which may include the case of joint without shear key or joint with beveled shear keys. Significant shear resistance is provided from cohesion and friction of the joint. By studying the results of this case, the probable significance of free slippage in a joint can be determined. In Case 5 the same assumptions are made for the shear keys as in Case 4 but with reduced shear resistance capacity. Case 6 is the same as Case 5 with a smaller friction angle. The reduced friction angle may be a result of water intrusion into the joints. In the discussions, for comparison Case 1 is chosen as the standard or reference case.

Of the large amount of results obtained, here only a few selected response time histories are presented and discussed to illustrate the typical behaviour of the dam. These are the responses at selected locations of the dam shown in Figure 4. However, the conclusions drawn from the results presented here are equally applicable to other response histories.

NUMERICAL RESULTS

Un-beveled shear keys

By comparing the results from Cases 2 and 3 with Case 1, it is found that the shear strength of the keys and the friction angle of the grouting material have negligible effects on the behaviour of the contraction joints in the dam considered. Since similar responses are obtained in Cases 2 and 3, only the results from Case 3 are presented here. In Figure 5 the response of the stream component of the relative displacement of the joint element at point B on the upstream face of the dam is presented. The two response time histories in the figure are practically the same except at time 7·4 s around the time when the peak ground excitation occurs. The same behaviour is observed in the time histories of other response quantities. These results indicate that as long as the joint faces remain engaged, sufficient resistance is provided by the shear keys to prevent shear slippage. The assumed shear keys in this case study are strong enough to prevent slippage even when the joints are fully open across the thickness of the dam.

Joint slippage

Cases 4–6 are analysed to investigate the effects of free shear slippage in joints with beveled shear keys and/or joints without shear keys. The results are presented in this section. A slip margin of 3 mm is assumed here for all three cases.

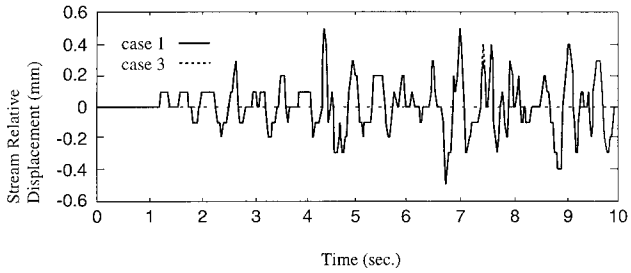

Figure 5. Stream component of relative displacement of joint at point B

Joint displacement time histories

Comparison of the results from Cases 1, 4 and 5 shows that the dam with no shear keys, or with beveled shear keys, has substantial shear slippage across the joints. Because of symmetry, there is no shear sliding motion at the crown middle section of the dam. Consequently, to illustrate the significance of this behaviour, the vertical, stream and normal components of the relative displacement of the joint element located on the upstream face of the dam at point C are plotted in Figure 6. The time histories shown in Figures 6(a) and 6(b) clearly indicate that shear slippage within the joint element occurs at five separate occasions, at 4·7, 6·8, 7·2, 8·8 and 9·8 s. At the instant of shear slippage, the joint opening exceeds the slip margin of 3 mm, as can be observed in Figure 6(c). The amount of slippage in the stream direction is one order of magnitude larger than that in the vertical direction. Similar behaviour can also be observed in the three relative displacement components of the contraction joint at point B on the upstream face of the dam.

From Figures 6(a) and 6(b), it is noted that although the primary cause of slippage in the contraction joint is the loss of shear engagement as a result of the opening of the joint beyond the slip margin, the strength of the shear key and the friction angle of the grout have significant influence on the behaviour of the dam. Although the effects of the latter parameters are less than that of free slippage, the results show that a difference of up to 20 per cent in the amount of maximum slippage can occur at the contraction joint. The amount of slippage in the stream component can be as high as 90 mm, which demonstrates the significance of beveled shear keys and their effect on the behaviour of the dam. Considering the assumed slip margin of 3 mm, and a side slope angle of 25° in a typical beveled shear key joint, the maximum permissible relative free slippage for such a key would be 6 mm, indicating that if the joint slips more than 6 mm, the shear key will then act as a restraining barrier against further sliding.

Figure 6(c) also shows that shear slippage can significantly affect the opening and closing behaviour of the joint. The maximum joint opening with shear slippage is 30 per cent higher than that in the case of no shear slippage. It is also observed that penetration between the two faces of the joints can reach 5·8 mm, due to the relatively small penalty parameter used in the analysis to alleviate the vibration noise problem and oscillation in the response. However, it may be argued that the penetration actually represents the contraction deformation of the grout material in the joint.

Furthermore, the results in Figure 6(c) demonstrate that slippage has little effect on the pattern of the joint opening and closing dynamic response. As joint slippage is a relatively instantaneous phenomenon, the contraction joint regains its full normal stiffness as soon as the joint faces come back to full engagement, and the dam structure resumes its original dynamic structural properties, vibrating about a new baseline due to the slippage.

To determine whether further reduction in friction angle, possibly due to the lubricating effect of intruding water, can have any effect on the slippage of the joints, the responses of Cases 5 and 6 presented in Figures 6(a) and 6(b) are compared. The reduction of the friction angle from 45 to 25° causes a small increase of about 3 per cent in the peak slippage.

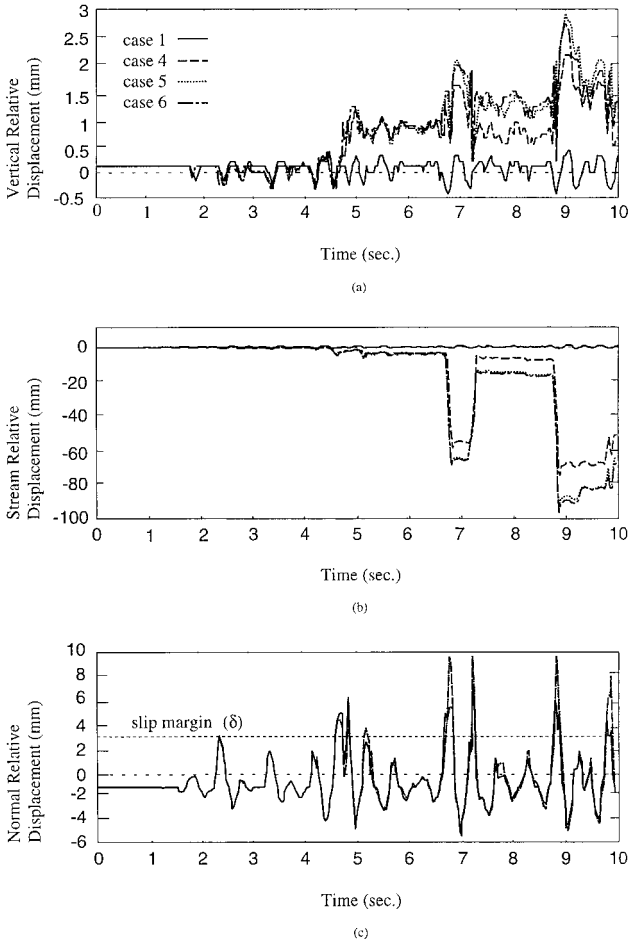

Figure 6. Relative displacements of joint at point C

To give an indication on the magnitude of the total displacement of the dam, the stream component of the total displacement at point C on the upstream face of the dam is plotted in Figure 7.

In general, the results indicate that slippage results in a permanent change to the geometry of the arch dam after the earthquake stops. This will affect the stress distribution in the dam and may have significant impact on the short- and long-term behaviour of the structure.

Joint stress time histories

The effect of joint opening on the stress distribution in arch dam has been studied by other researchers, hence the effect of sliding of the joint is presented in this section. Figure 8 shows the time histories of the joint stresses in the vertical, stream and normal directions at point C on the upstream face from Cases 1, 4 and 5. The results indicate that when the normal relative displacement of the joint exceeds the slip margin, there is no shear transfer across the joint while at the same time, the normal stress of the joint also reduces to zero. The effect of shear slippage is clearly demonstrated by the shifts in the stress responses at the instants of slippage. Sliding of the joint generally causes significant increase in the peak response of the vertical and stream stresses, whereas the normal stress is negligibly affected. This is because the normal stress is largely controlled by the joint opening and closing behaviour. Comparing the results from Cases 4 and 5,

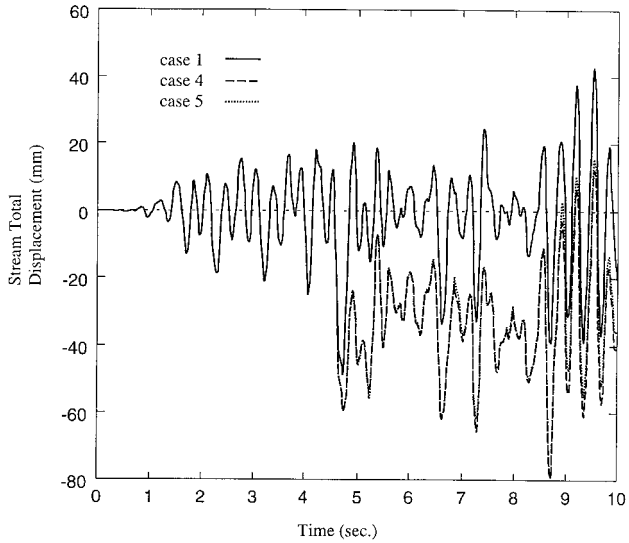

Figure 7. Stream component of total displacement of joint at point C

it is observed that reducing the apparent cohesion strength of the joint results in substantial changes to the joint shear stresses, including stress reversal. Although not shown here, the results of Case 6 are essentially the same as those in Case 5, indicating that a smaller friction angle for the joint has negligible effect on the behaviour of the dam.

Results from the present study confirm the observations by other researchers that the stresses in the joint can have significant effects on the integrity of the concrete in the regions adjacent to the contraction joints, especially when the joints are only partially open. Furthermore, as joint opening is usually confined to the upper level of the dam, shear slippage generally occurs at the upper part of the dam.

Stress contours

To investigate the effect of slippage on the overall behaviour of the dam, envelopes of the maximum arch and cantilever stresses on the upstream and downstream faces of the dam are determined. Figure 9 shows the envelopes of the maximum cantilever stresses on the downstream face of the dam for Cases 1, 4, and 5. It is observed that free slippage causes very significant changes in the stress envelope contour pattern, particularly at the upper levels of the dam where the maximum cantilever stress is almost doubled from 6 to 12 MPa, whereas the effect on the maximum arch stress is smaller, as can be noted in Figure 10. The stress envelope results clearly indicates that the cantilever stress is more significantly affected by shear slippage than the arch stress. Consequently, the slippage of the joints may lead to over stress of the dam in the cantilever direction.

CONCLUSIONS

A complete joint constitutive model that can simulate both the opening–closing and shear slippage non-linear effects, as well as the shear key effects, is formulated and is subsequently used in a finite element program to study the non-linear effects of contraction joints movements on the seismic response of a typical arch dam. The proposed joint constitutive model considers the coupling and elastoplastic behaviour of the normal and shear displacements at the joint under the closed state. In the open state, the constitutive model accounts for the restraining effect of the shear key in the tangential direction when the normal relative displacement of the joint is less than the height or slip margin of the key, and the free sliding behaviour when the normal

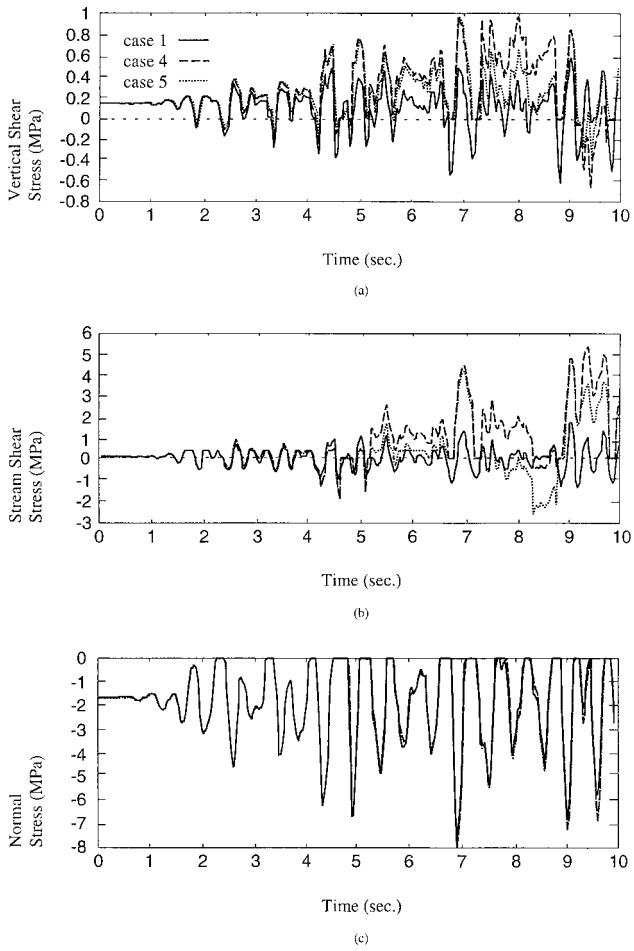

Figure 8. Joint stresses at point C

displacement exceeds the slip margin. The proposed joint model has been verified by numerical examples. The significance and contribution of the joint modelling parameters of slip margin, shear key strength and friction property of the grout material in the joint to the seismic behaviour of an arch dam have been studied in a parametric investigation.

Results of the analysis show that shear slippage across the contraction joints can cause very important changes in the displacement and stress fields of an arch dam. The primary cause of the changes are the opening of the joints beyond the allowable slip margin. Shear slippage at the joint faces causes permanent changes in the displacement field of the dam resulting in permanent changes in the stress pattern of the structure, which may have a significant impact on the short- and long-term behaviour of the dam. Since joint opening is most likely to be restricted to the upper parts of the dam, shear slippage will also occur in those areas. Shear keys, whether beveled or unbeveled, are very efficient barriers against shear slippage. However, in the case of the beveled shear keys, there is still a possibility of free shear slippage. Although the allowable slip margin is the dominant factor affecting the shear slippage behaviour, the bearing or shear strength of the keys and the friction angle of the grouting material can also have some effect on the behaviour of the dams in case of dams without shear keys, or with beveled shear keys. Generally, in case of contraction joints with

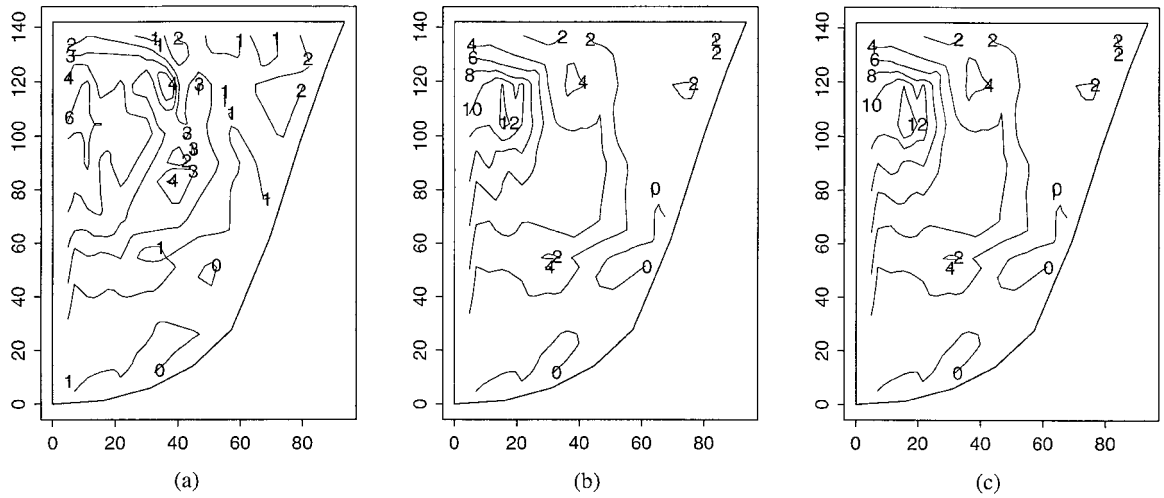

Figure 9. Envelopes of maximum cantilever stresses for: (a) Case 1; (b) Case 4; (c) Case 5

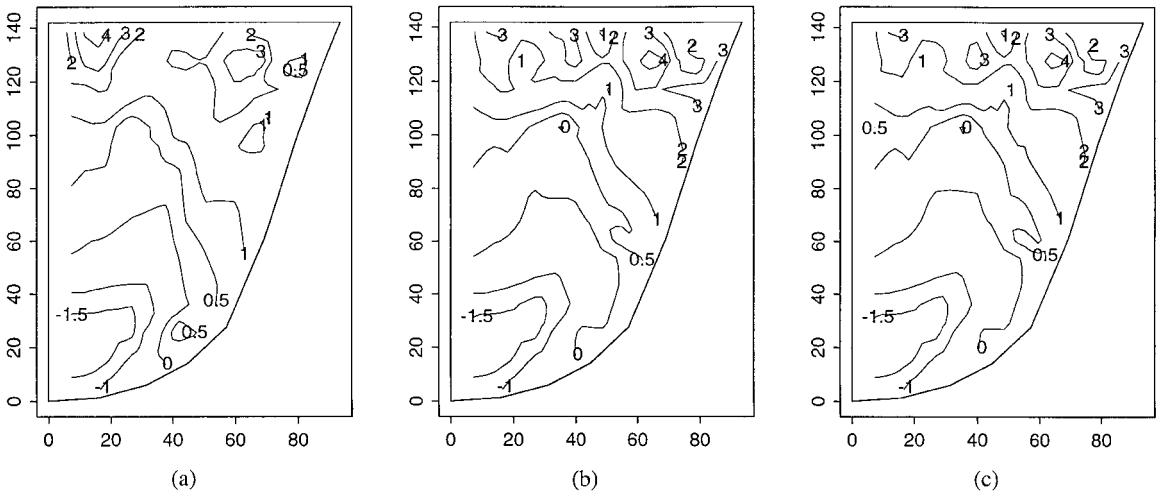

Figure 10. Envelopes of maximum arch stresses for: (a) Case 1; (b) Case 4; (c) Case 5

no shear keys, the lower parts of the dam do not experience any slippage and the stress distribution in those areas is not affected.

It is noted here that the above observations are obtained for full reservoir, the influences of the reservoir content and other parameters on the earthquake response of arch dams, including details of the shear key geometry, degradation of the shear key strength from damage and mismatch, require further investigation. Furthermore, numerical procedures should be developed to improve the efficiency and stability of the joint opening-sliding interface model.

ACKNOWLEDGEMENTS

This research was supported by grants from the Natural Sciences and Engineering Research Council of Canada and by the support of the Ministry of Higher Education of Iran to B. Noruziaan. These supports are gratefully

acknowledged. The authors would also like to thank Professor G. Fenves of the University of California at Berkeley for providing the computer program ADAP88, which formed the backbone of the program developed in this study.

REFERENCES

1. R. W. Clough, J. M. Raphael and S. Mojtahedi, 'ADAP : a computer program for static and dynamic analysis of arch dams', *Report No. EERC 73-14*, Earthquake Engineering Research Center, University of California, Berkeley, CA, 1973.
2. J. F. Hall and A. K. Chopra, 'Dynamic analysis of arch dams including hydrodynamic interaction', *J. Engng. Mech. Div ASCE* **109**, 149–167 (1983).
3. K. L. Fok and A. K. Chopra, 'Earthquake analysis of arch dams including dam-water interaction, reservoir boundary absorption, and foundation flexibility', *Earthquake Eng. Struct. Dyn.* **14**, 55–184 (1986).
4. K. L. Fok and A. K. Chopra, 'Hydrodynamic and foundation flexibility effects in earthquake response of arch dams', *J. Engng. Mech. Div ASCE* **112**, 1810–1828 (1986).
5. K. L. Fok and A. K. Chopra, 'Water compressibility in earthquake response of arch dams', *J. Engng. Mech. div ASCE* **113**, 958–975 (1987).
6. Y. Ghanaat and R. W. Clough, 'EADAP: enhanced arch dam analysis program', *Report No. EERC 89-07*, Earthquake Engineering Research Center, University of California, Berkeley, CA, 1989.
7. S. B. Kojić and M. D. Trifunac, 'Earthquake stresses in arch dams. I: Theory and antiplane excitation', *J. Engng. Mech. Div ASCE* **117**, 532–552 (1991).
8. S. B. Kojić and M. D. Trifunac, 'Earthquake stresses in arch dams. II: Excitation by SV-, P-, and Rayleigh waves', *J. Engng. Mech. Div ASCE* **117**, 553–574 (1991).
9. A. K. Chopra, 'Earthquake analysis, design, and safety evaluation of concrete arch dams', *Proc. 10th World Conf. on Earthquake Engineering*, Balkema, Rotterdam, 1992, pp. 6763–6772.
10. L. Bolognini, P. Masarati, A. Dusi and C. Galimberti, 'Arch dams non-linear seismic analysis using a joint finite element', *Proc. 10th World Conf. on Earthquake Engineering*, Balkema, Rotterdam, 1992, pp. 4705–4710.
11. J. R. Mays and L. H. Roehm, 'Effect of vertical contraction joints in concrete arch dams', *Comput. Struct.* **47**, 615–627 (1993).
12. H. Tan and A. K. Chopra, 'Earthquake analysis and response of concrete arch dams', *Report No. EERC 95-07*, Earthquake Engineering Research Center, University of California, Berkeley, CA, 1995.
13. A. Niwa and R. W. Clough, 'Nonlinear seismic response of arch dams', *Earthquake Engng. Struct. Dyn* **10**, 267–281 (1982).
14. M. J. Dowling and J. F. Hall, 'Nonlinear seismic of arch dams', *J. Engng. Mech. Div ASCE* **115**, 768–789 (1989).
15. L. Taskov and D. Jurukovski , 'Analytical studies of non-linear behaviour of arch dams using shaking table test results of an arch dam fragment', *Proc. 9th World Conf. on Earthquake Engineering*, Tokyo, Japan, 1988, pp. 385–390.
16. B. Weber, J. M. Hohberg and H. Bachmann, 'Earthquake analysis of arch dams including joint nonlinearity and fluid-structure interaction', *Earthquake Resistant Construction and Design*, Balkema, Rotterdam, 1990, pp. 348–358 .
17. J. M. Hohberg, 'Seismic arch dam analysis with full joint non-linearity', *Proc. Int. Conf. on Dam Fracture*, Denver, Colorado, 1991, pp. 61–75.
18. G. L. Fenves, S. Mojtahedi and R. B. Reimer, 'ADAP88 : a computer program for nonlinear earthquake analysis of concrete arch dams', *Report No. EERC 89-12*, Earthquake Engineering Research Center, University of California, Berkeley, CA, 1989.
19. G. L. Fenves, S. Mojtahedi and R. B. Reimer, 'Effect of contraction joints on earthquake response of an arch dam', *J. Struct. Engng.* **118**, 1039–1055 (1992).
20. G. L. Fenves, S. Mojtahedi and R. B. Reimer, 'Parameter study of joint opening effects on earthquake response of arch dams', *Report No. EERC 92-05*, Earthquake Engineering Research Center, University of California, Berkeley, CA, 1992.
21. A. M. Crawford and J. H. Curran, 'A displacement discontinuity approach to modelling the creep behaviour of rock and its discontinuities', *International J. Numer. Anal. Meth. Geomech.* **7**, 245–268 (1983).
22. C. S. Desai and B. K. Nagaraj, 'Modelling for cyclic normal and shear behaviour of interface', *J. Engng. Mech. Div ASCE* **114**, 1198–1217 (1988).
23. A. Gens, I. Carol and E. E. Alonso, 'A constitutive model for rock joints formulation and numerical implementation', *Comput. Geotech.* 3–20 (1990).
24. C. S. Desai and K. L. Fishman, 'Plasticity-based constitutive model with associated testing for joints', *Int. J. of Rock Mech. Mining Sci. Geomech. Abstracts* **23**, 15–26 (1991).
25. J. M. Hohberg, 'Concrete joints', in: *Mechanics of Geomaterial Interfaces*, A. P. S. Selvadurai and M. Boulon (eds), Elsevier, Amsterdam, 1995.
26. S. Malla and M. Wieland, 'Effect of friction in vertical contraction joints of arch dams', *Proc. SwissNCOLD/ICOLD Symp. on Research and Development in the Field of Dams*, Crans-Montana, Switzerland, September 7–9, 1995.
27. J. Kuo, 'Fluid–structure interactions: Added mass computations for incompressible fluid', *Report No. EERC 82-09*, Earthquake Engineering Research Center, University of California, Berkeley, CA, 1982.

